DETERMINATION OF THE CONFORMATION OF SPECIFIC RESIDUES IN A MODEL PEPTIDE BY ^{13}C ISOTOPE-EDITED ATR-FTIR IN REGULAR WATER

by

Sneha Potana

A Thesis Submitted in Partial Fulfillment

of the Requirements for the Degree of

Master of Science in Chemistry

Middle Tennessee State University

2013

Thesis Committee:

Dr.Chengshan Wang, Major Professor

Dr. Ngee-Sing Chong

Dr. Keying Ding

I dedicate this research work to my family.

ACKNOWLEDGMENTS

I would like to express my sincere gratitude to my research advisor, Dr. Chengshan Wang, for his excellent support and continuous guidance throughout my research. Also, I extend my sincere word of thanks to Dr. Ngee-Sing Chong and Dr. Keying Ding for their support by serving in my committee and giving me valuable suggestions. I would like to acknowledge Dr. Leblanc of the University of Miami for his assistance with ATR-FTIR measurements.

I would greatly thank my parents for their enormous love, constant motivation and moral support. I am grateful to my sisters, Swetha and Silpa, who have always been there whenever I needed them the most. I would not have been here without their guidance, blessings and support.

I would like to thank my lovely friends, Hari Priya, Tejaswini, Sowmya, Mamatha, Divya for being with me through thicks and thins of life, I find myself lucky to have friends like them in my life. I would like to thank my wonderful roommates, Archana and Kavya, for providing a homely and cheerful environment and constantly encouraging me throughout my research. My heartfelt thanks to my friends, Amrita, Anita, Anup, Tuphan, Ameen, Kateryna, Kiran for making my life at MTSU as the most memorable and pleasant one.

Last but not least, my acknowledgment goes to the all the faculty members and staff in the Department of Chemistry at MTSU for their help and support during my research project

ABSTRACT

Determination of protein structures has attracted extensive scientific attention. IR spectroscopy using traditional liquid cells has been reported to address the structure in a model peptide of sequence Ac-YAAKAAAKAAAAKAAH-NH_2 (pep17) with ^{13}C isotopic labels in deuterated water (D_2O). Although similar to regular water, D_2O is not physiologically equivalent to H_2O in the aqueous matrix of cells and tissues. Therefore, peptide studies in D_2O may not yield true peptide conformations. Here, ^{13}C isotope-edited FTIR was applied on pep17 in H_2O using the Attenuated Total Reflection (ATR) technique. The peak of ^{13}C labeled residues in α-helix appears at 1602 cm^{-1}, which can be used as a fingerprint peak of α-helix for the ^{13}C labeled residue. By the presence or absence of peak at 1602 cm^{-1}, conformation of specific residues in the peptide was determined. For the first time, the elucidation of the secondary structure of the pep17 has been demonstrated in H_2O.

TABLE OF CONTENTS

PAGE

LIST OF FIGURES

FIGURE **PAGE**

LIST OF TABLES

TABLE **PAGE**

LIST OF SCHEMES

SCHEME **PAGE**

CHAPTER I

INTRODUCTION

1.1 Structural Biology

Proteins are complex biological macromolecules, consisting of chains of amino acids covalently linked by amide bonds.[1-4] All the proteins found in biological systems are composed of 20 different amino acids. As shown in Figure 1, an amino acid consists of an alpha carbon which is bonded to amino group, carboxyl group, hydrogen atom and a R group. R group is also called residue group. Amino acids are distinguished based on the structure of R group (Table 1).

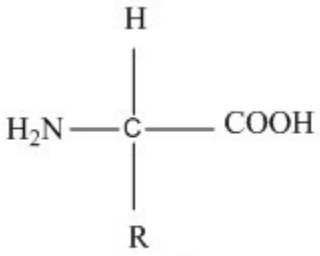

Figure 1: Structure of an amino acid.

Essential to life processes, proteins perform a variety of functions, including catalyzing metabolic reactions,[5-9] replicating DNA,[10, 11] responding to stimuli.[12, 13] On the other hand, the malfunction of proteins has been linked to many diseases.[5, 7, 8, 14-17] Therefore, the elucidation of protein structure will not only help biochemists understand

Table 1: Structure of R groups of amino acids

Amino acid	Abbreviations		Structure of R group
Alanine	Ala	A	$-CH_3$
Arginine	Arg	R	$-(CH_2)_3-NH-C(NH_2)=NH$
Asparagine	Asn	N	$-CH_2-CO-NH_2$
Aspartic acid	Asp	D	$-CH_2-COOH$
Cysteine	Cys	C	$-CH_2-SH$
Glutamine	Gln	Q	$-(CH_2)_2-CO-NH_2$
Glutamic Acid	Glu	E	$-(CH_2)_2-COOH$
Glycine	GlY	G	-H
Histidine	His	H	$-CH_2C_3H_3N_2$
Isoleucine	Ile	I	$-CH(CH_3)-CH_2-CH_3$
Leucine	Leu	L	$-CH_2-CH-(CH_3)_2$
Lysine	Lys	K	$-(CH_2)_4NH_2$
Methionine	Met	M	$-(CH_2)_2-S-CH_3$
Phenylalanine	Phe	F	$-CH_2-C_6H_5$
Proline	Pro	P	$-CH(CH_2)_3NH$
Serine	Ser	S	$-CH_2-OH$
Threonine	Thr	T	$-CH(OH)-CH_3$
Tryptophan	Trp	W	$-CH_2-C_8H_6N$
Tyrosine	Tyr	Y	$-CH_2-C_6H_5-OH$
Valine	Val	V	$-CH-(CH_3)_2$

how proteins work *in vivo* but also provide pathological information about many diseases. As a consequence, structural biology which focuses on the elucidation of the protein structure contributed to many areas of biochemical research.[18-21] For example, the determination of the structure of the photosynthesis center was recognized with the chemistry Nobel Prize in 1988[18] and the 2009 Nobel Prize was awarded to Venkatraman Ramakrishnan, Thomas A. Steitz, and Ada Yonath for the elucidation of the structure of ribosome.[8, 19, 20]

1.2 Protein Structure

1.2.1 Primary Structure

Amino acids are covalently linked together by an amide bond (i.e., CO-NH), formed between the amine group of one amino acid and the carboxyl group of the adjacent amino acid.[3] A chain of amino acids connected by amide bonds is referred to as a polypeptide chain. The two termini of a polypeptide chain are called N-terminus (it has free amine group) and C-terminus (it has free carboxylic acid group). Polypeptide is usually written from N-terminus to C-terminus. An example of protein primary structure is given by the following sequence of β-amyloid which is hallmark protein of Alzheimer's disease:

DAEFRHDSGYEVHHQKLVFFAEDVGSNKGAIIGLMVGGVVIA

Each letter represents one amino acid according to the designation given in Table 1.

1.2.2 Secondary Structure

The secondary protein structure is the specific geometric shape caused by the intra-molecular and inter-molecular hydrogen bonding of amide groups. Typical secondary

structures (also called as conformations) are α-helix, β sheets, and random coils.[22-24] Random coil structure is also called unstructured conformation, in which the polypeptide chain is well dissolved in the aqueous solution and moves freely in the aqueous environment.

As the most common secondary structure, the α-helix looks like a spring as shown in Figure 2. α-Helix is characterized by the intra-molecular hydrogen bonds between the amino group of one amino acid and the carbonyl group of other amino acid located 3~4 residues away along the polypeptide chain.[23] These hydrogen bonds are usually present parallel to the helical axis. The α-helix is usually right handed and contains approximately 3.6 amino acid residues per turn. Formation of hydrogen bonds creates helical structure of polypeptide chain, as a result side chains of amino acids protrude out of the helix.

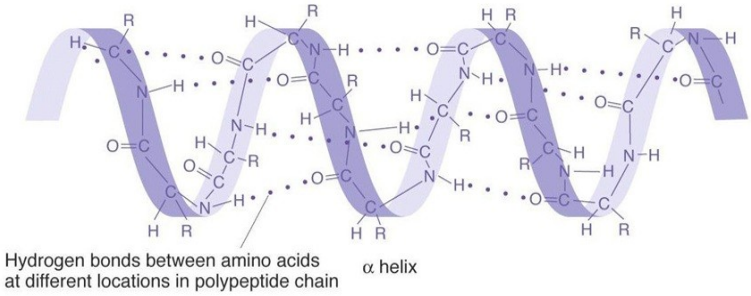

Figure 2: Structure of an α-helix.

The structural units of β sheets are strands. It is a fully extended structure characterized by multiple strands arranged side-by-side.[22] Each β sheet contains 6 to 22 strands. Side chains are present above and below the plane of polypeptide chain. Inter-

strand hydrogen bonds are formed between the carbonyl oxygen of one chain and the amide hydrogen of other chain. β sheet includes two types, namely, parallel and anti-parallel sheets. In a parallel sheet, two strands run in the same direction. In an anti-parallel sheet, the neighboring strands run in opposite direction. For example, if one strand runs from N-terminus to C-terminus, the neighboring strand runs from C-terminus-N-terminus. They are shown in Figure 3.

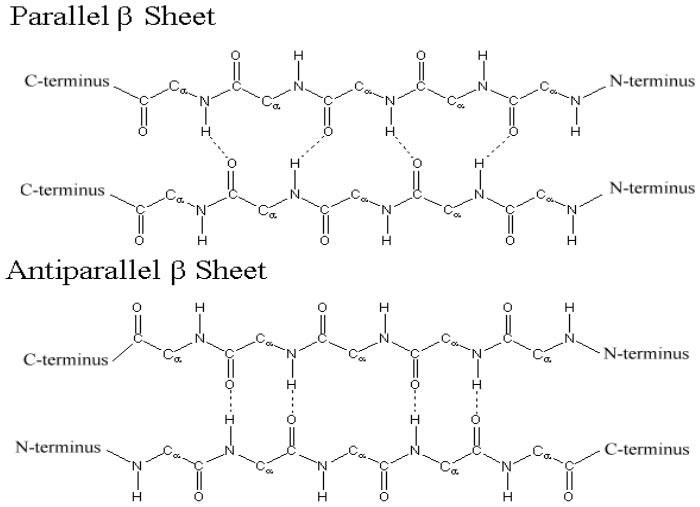

Figure 3: Parallel and Anti-parallel β sheet.

1.2.3 Tertiary Structure

Tertiary structure arises when secondary structure elements pack tightly to form the well-defined 3D structure.[25, 26] It is usually stabilized by four forces, hydrophobic forces, covalent bond, Van der Waals interaction, and hydrogen bonds. Among these four forces, hydrophobic interactions play an important role in stabilizing the secondary structure. To determine protein structure, various techniques have been developed and the major techniques are described in the following sections.

1.3 Techniques to Clarify Protein Structure

1.3.1 X-ray Crystallography

X-ray crystallography is the most widely used method to address protein structure and the detailed protein structure can be determined in atomic level.[27, 28] Most of the protein structures in protein data bank were determined by this method.[1] However, this technique has some drawbacks. First, proteins have to be isolated as a single crystal structure for X-ray measurement and yet there is not a common crystallization method that can be applied to all proteins. Many proteins do not readily form single crystal structures. This includes, β-amyloid protein (Aβ) which contains 40-42 amino acids and is the hallmark protein of Alzheimer's disease. Despite the efforts for producing the single crystal structure of Aβ for more than 20 years, no report has been published about the single crystal structure of Aβ. Second, artificial solvents are needed to facilitate the crystallization of proteins. In addition, crystalline structure presents a static environment that is not favorable to study of proteins because they are only functional in dynamic aqueous environment.

1.3.2 NMR Spectroscopy

Another powerful technique is multi-dimensional NMR. The advantage of NMR spectroscopy is that it could determine the structure in aqueous environment that preserves the function of proteins.[29-33] However, deuterated water or heavy water (D_2O), which does not accurately represents the aqueous biological systems, needs to be added into the solution to lock the magnetic field of NMR. Furthermore, measurement of the NMR spectra of proteins needs a long data acquisition time and the interpretation is

complicated.[29-33] This makes it impossible for NMR to determine the protein structure with short lifetime of less than 10 hours.[33] As mentioned above, it has been reported that the small aggregates (i.e., oligomers) of Aβ are toxic to neuronal cells in the brain and the oligomer's lifetime is usually around one or several hours.[33] Therefore, faster methods for determining the protein structure have to be developed. The two mostly widely used techniques are Circular Dichroism (CD) and IR spectroscopy.

1.3.3 Circular Dichroism (CD) Spectroscopy

There is a long history of CD studies of peptides and proteins in the biochemical and biophysical science.[24, 34-39] CD utilizes circular polarized light and it is of two types: namely, Left Circular Polarized (LCP) light rotating counter clockwise and Right Circular Polarized (RCP) light rotating clockwise. CD refers to the difference in the absorption of LCP and RCP (Figure 4).

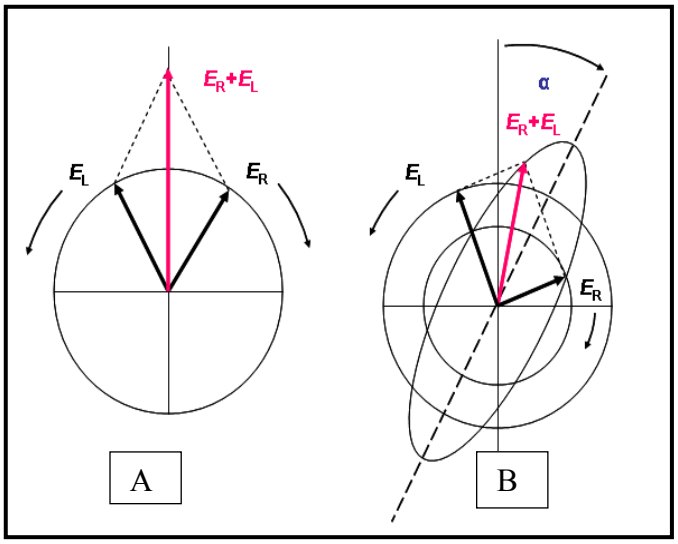

Figure 4: Diagrams showing the combination of right and left circular polarized light.

In Figure 4, if two waves have the same amplitude, the result is plane-polarized light (Figure 4 A), if their amplitudes differ, the result is elliptically polarized light, with unequal contributions of right and left circular polarized light to give molar ellipticity (θ) (Figure 4 B).

If the LCP and RCP are absorbed to different extents by a sample (such as peptides which contains chiral atoms), CD signal (ΔA) will appear as following equation

$$\Delta A = A_L - A_R \qquad \text{Equation 2-1}$$

where ΔA is the difference between absorbance values of LCP and RCP light. It can also be expressed by, applying Beer's law, as:

$$\Delta A = (\varepsilon_L - \varepsilon_R)Cl \qquad \text{Equation 2-2}$$

where ε_L and ε_R are the molar extinction coefficients for LCP and RCP light, C is the molar concentration and l is the path length in centimeters. Then,

$$\Delta\varepsilon = \varepsilon_L - \varepsilon_R \qquad \text{Equation 2-3}$$

where Δε is the molar circular dichroism. Although ΔA is usually measured as CD signal, most measurements are reported in degree of ellipticity (molar ellipticity) with units of degrees-cm^2/dmol for historical reasons

CD is very sensitive to protein conformation and is a fast method for monitoring structural changes in protein, because the measurement of CD can be accomplished in several minutes. Due to the large number of carbonyls (C=O which absorbs intensively around 200 nm) in the amide bonds, proteins usually show strong CD signals between 260 and 180 nm.[24, 38, 39] Since the carbonyls are arranged differently in conformations

(such as α-helix, β sheets, and unstructured conformation), every secondary structure shows its distinct patterns in CD spectrum.[34, 37]

The far-UV CD spectrum of the α-helix conformation has two characteristically negative peaks at 222 nm and 208 nm and one positive peak at 192 nm. The far-UV CD spectrum of β-sheet conformation exhibits a positive peak at 196 nm and a negative peak at 215 nm. As for the unstructured conformation, only one negative peak at 199 nm will be detected (Figure 5).[34, 37] Similarly, every conformation can also show their distinct patterns in the FTIR spectroscopy.

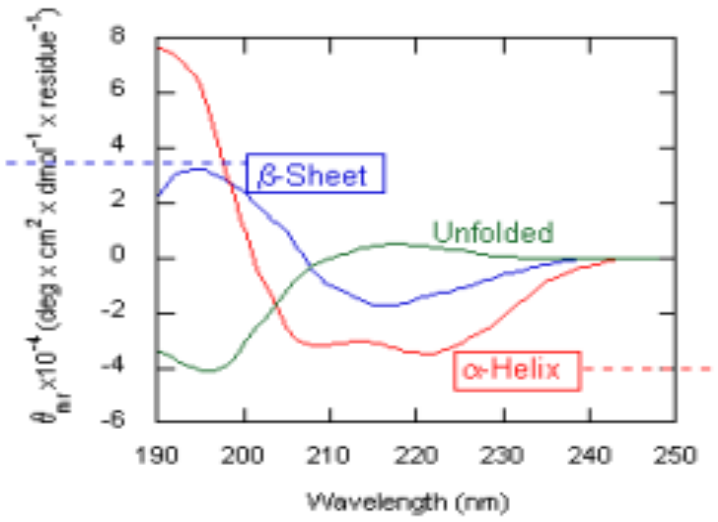

Figure 5: CD spectra of secondary structural elements.

1.3.4 FTIR Spectroscopy

Infra-red (IR) spectroscopy is another widely used technique for the analysis of secondary structures of the peptides.[24, 38-47] The main advantage of IR spectroscopy over other techniques is that it can be applied to a wide range of sample types including powders, crystals, solid dosage forms, crystals. Furthermore, the amount of sample

required for analysis is very small. Even the membrane proteins can be analyzed by this method.[24, 38, 39, 43, 46, 47] After the development of Fourier Transform Infra-Red (FTIR) spectrometers, spectra of high accuracy were obtained and the signal-to-noise ratio of instrument was also improved. In addition, the acquisition of an FTIR spectrum requires only several seconds to several minutes, depending on the number of co-added scans. Thus, FTIR spectroscopy has become a powerful tool in conformational analysis of proteins/peptides, especially for the detection of transitional conformation change under varying environmental conditions of temperature or pH.

In FTIR spectroscopy, peptides/proteins absorb the infrared radiation and give rise to nine characteristic bands, namely Amide A, B, and I throughVII.[24, 38, 39, 43, 54] Frequencies and description of these amide bands are shown in Table 2.[54] Among all these bands, Amide I and Amide II bands are found to be the most prominent bands in the spectra of proteins. Amide I band is found around 1600-1700 cm^{-1} and it is mainly associated with C=O stretching vibration (over 85 %). Amide II band is related to the N-H bending vibration (40-60%) and from C-N stretching vibration (18-40%) and is found to be less sensitive to the conformations of protein when compared to Amide I band. All the other bands are susceptible to spectral overlap with IR absorption bands from different vibrations. Consequently, they are less useful in protein conformational studies.

Table 2: Characteristic infrared bands of peptide linkage.[54]

Designation	Approximate Frequency (cm^{-1})	Description
Amide A	3300	NH stretching
Amide B	3100	NH stretching
Amide I	1600-1690	C-O stretching
Amide II	1480-1575	CN stretching, NH bending
Amide III	1229-1301	CN stretching, NH bending
Amide IV	625-767	OCN bending
Amide V	640-800	Out-of-plane, NH bending
Amide VI	537-606	Out-of-plane, C-O bending
Amide VII	200	Skeletal torsion

In the Amide I region (1600-1700cm^{-1}), each type of secondary structure (α-helix, β sheet, or unstructured conformation) gives rise to unique frequency due to the different hydrogen bonding pattern among them.[38, 39, 46] Different types of secondary structures and their frequencies are shown in Table 3.[46] For example, unstructured conformation shows a peak at ~1640 cm^{-1} in Amide I band and the peak of β sheet is ~1630 cm^{-1}. As for α-helix, the peak position is affected by the length of helix. For long helix with more than 20 residues, the peak will appear around 1648 cm^{-1} and move to higher frequency when the helix becomes shorter.

Table 3: Characteristic Amide I frequencies of protein secondary structure

Frequency (cm^{-1})	Assignment
1690-1680	β sheet structure
1666-1659	α-helix (short)
1657-1648	α-helix (long)
1645-1640	Random coil
1630-1620	β sheet structure

1.3.5 Quantitative Estimation of Secondary Structures in Certain Proteins

As mentioned in section 1.3.1 and 1.3.2, x-ray crystallography can provide the structural information in atomic level but required target proteins to form single crystal. Multi-dimensional NMR can analyze the proteins structure in solution with high resolution, but the measurement is quite time-consuming. Therefore, quantitative estimation of secondary structures of protein has been reported using CD and FTIR. The basic assumption of the quantitative estimation of secondary structure of protein is that proteins/peptides are a linear sum of a few fundamental secondary structural elements and percentage of each element is related to spectral intensities.

As for CD spectroscopy, software programs such as CONTIN, CDSSTR, SELCOM, and CD-Pro have been developed for calculating the percentage of every secondary structure in proteins by CD spectroscopy.[35, 37-39, 48] For example. Dr. Wang *et al.* have shown that the CD spectra of aequorin (a bio-fluorescence protein) are affected by pH (Figure 6). The negative peaks at 208 nm and 222 nm reach the maximum at pH 7.6, because increasing or decreasing the pH values will decrease the peak intensity. This indicates that aequorin contains the highest percentage of α-helix at pH 7.6. To get more

detailed information, the CD spectra were analyzed by CD-Pro and the results are shown in Table 4. When the pH is increased, the percentage of α-helix decreases and that of unstructured conformation increases. Thus, the increase of pH changes some α-helix in aequorin to unstructured conformation. When pH is decreased, the percentage of β sheet increases, which indicates the transformation of some α-helix in aequorin to β sheet.[38]

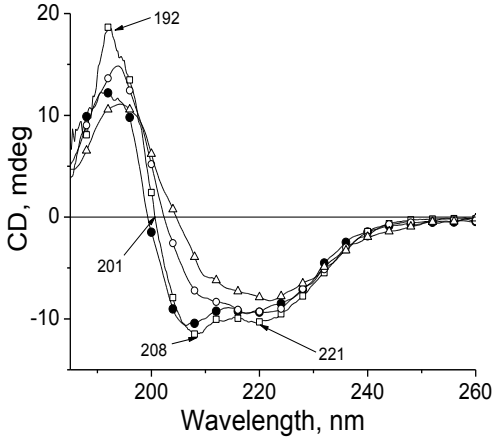

Figure 6: CD spectra of aequorin at the concentration of 0.1 mg.ml^{-1} under different pH values, -●- 9.0, -□- 7.6, -○- 4.8, -Δ- 4.0.

Table 4: Percentage of the three conformations of aequorin secondary structures at different pH values

pH	α-helix (%)	β sheet(%)	Unstructured (%)
9.0	32.8	14.8	53.1
7.6	37.8	13.5	48.9
4.8	30.9	20.1	49.3
4.0	23.9	27.8	47.5

Similarly, curve fitting procedure can be applied to FTIR spectra for the deconvolution of spectral overlap. The percentage of secondary structures can be quantitatively estimated after the resolution enhancement of Amide I spectra by Fourier self-deconvolution technique. Dong *et al.* reported the distribution of secondary structures determined from the Amide I spectra of globular proteins, which was nearly identical to the amount computed from crystallographic data.[49]

Although overall content of secondary structures in proteins/ peptides was investigated by IR and CD spectroscopy, structural elements (α-helix, β sheets) cannot be assigned to specific amino acid residues in polypeptide sequence. Therefore, a new technique called ^{13}C isotope-edited infrared spectroscopy has been used to improve the low resolution results of traditional CD or FTIR to "medium resolution"(i.e., in residue level).[49]

1.3.6 ^{13}C Isotope-Edited IR Spectroscopy

^{13}C Isotope-edited IR spectroscopy has been reported in 1991[50-53] and used in the study of several proteins and peptides for probing the structures of particular regions within a protein, elucidating the protein-protein and protein-peptide interactions, and determining the orientation of peptides and proteins in phospholipid membranes.[50-53] Later, it was applied in the study of the synthesized model peptides and was reported to address the secondary structure information in residue level in deuterated water.[54-57] This job cannot be accomplished by either traditional IR or CD spectroscopy. The proof-of-principle test of ^{13}C isotope-edited IR spectroscopy was accomplished on a model peptide with both α-helix and unstructured conformations. A peptide with sequence Ac-

YAAKAAAKAAAAKAAH-NH_2 (Ac means C-terminus and NH_2 indicates the N-terminus) has been shown to be a mixture of unstructured conformation and α-helix in D_2O.[56] Dr. Decatur and coauthors have synthesized four double ^{13}C labeled peptides (Scheme 1) by using ^{13}C-labels to replace the regular carbons of the carbonyl group in alanine in the peptide sequence, starting from C-terminus to N-terminus

Ac-Y<u>AA</u>KAAAAKAAAAKAAH-NH_2 (L1)

Ac-YAAKA<u>AA</u>AKAAAAKAAH-NH_2 (L2)

Ac-YAAKAAAAKA<u>AA</u>AKAAH-NH_2 (L3)

Ac-YAAKAAAAKAAAAK<u>AA</u>H-NH_2 (L4)

Scheme 1: Sequence of the ^{13}C double labeled peptides of pep 17. The carbonyls of underlined alanine residues are replaced by ^{13}C labels

When the temperature is increased to 45 °C, CD results showed that almost all of the residues in the peptide are in unstructured conformation.[56] The ^{13}C labels in the peptide do not change this property and the Amide I band of the ^{13}C labeled carbonyls (^{13}C=O) in unstructured conformation is identical to that of regular Amide I band (at 1640 cm^{-1} in D_2O), because carbonyls interact with solvent molecules very well. When the ^{13}C labeled residue is in α-helix, the Amide I band of ^{13}C labeled residue (referred as Amide I' band in the following) moves to 1602 cm^{-1}, which is different from the regular Amide I band of α-helix at 1630 cm^{-1} in D_2O.

At 0 °C, the CD results showed that lots of residues in the peptide transform to α-helix but several residues remain the unstructured conformation. Which residues still remain in the unstructured conformation? To address this question, the FTIR spectra of

L1 to L4 in D_2O were measured and the results were shown in Figure 7. As for unlabeled peptide, no Amide I' band was detected. For L1, L2, and L3, the Amide I' band was detected at 1602 cm^{-1}, which means that residues 2, 3, 6, 7, 11, and 12 were transformed to α-helix at 0 °C. However, Amide I' band does not appear in L4 even at 0 °C. This indicates that residues 15 and 16, which are ^{13}C labeled in L4, were still in unstructured conformation at 0 °C. By observing the presence or absence of Amide I' band in the FTIR spectrum of selectively ^{13}C labeled peptide, the conformation of every residue can be determined by the technique of ^{13}C isotope-edited FTIR spectroscopy.

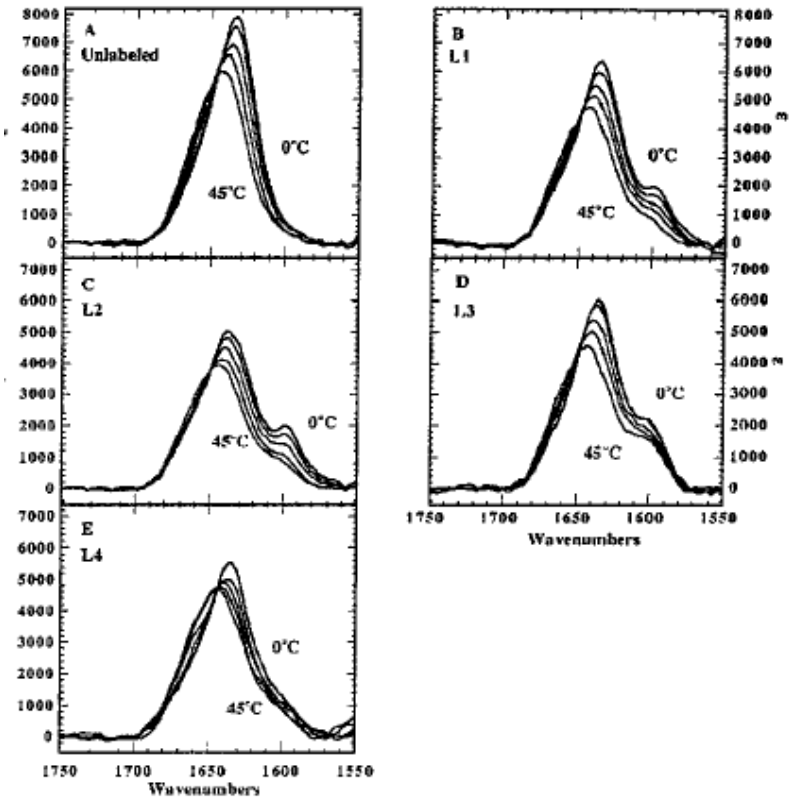

Figure 7: FTIR spectra of labeled and unlabeled pep17 at 0, 15, 25, and 45 °C. (A) unlabeled pep17, (B) L1, (C) L2, (D) L3, and (E) L4

1.3.7 Challenges of ^{13}C Isotope-edited FTIR Spectroscopy

It is worth noting that all of the ^{13}C isotope-edited FTIR spectroscopy was performed in D_2O, not H_2O. Although D_2O and water are quite similar, their physiological properties are quite different.[58-60] Proteins can exhibit their function only in normal water.[58, 61] In addition, D_2O is also expensive and harmful to health.[58] Therefore, further application of ^{13}C isotope-edited FTIR spectroscopy of proteins/peptides in H_2O is important. However, since H_2O has intensive absorption around 1610 cm^{-1} (Figure 8)[62] which will interfere with the observation of all the peaks of α-helix and β sheet, direct transmission measurement of FTIR spectra of peptides/proteins in H_2O solution will fail.

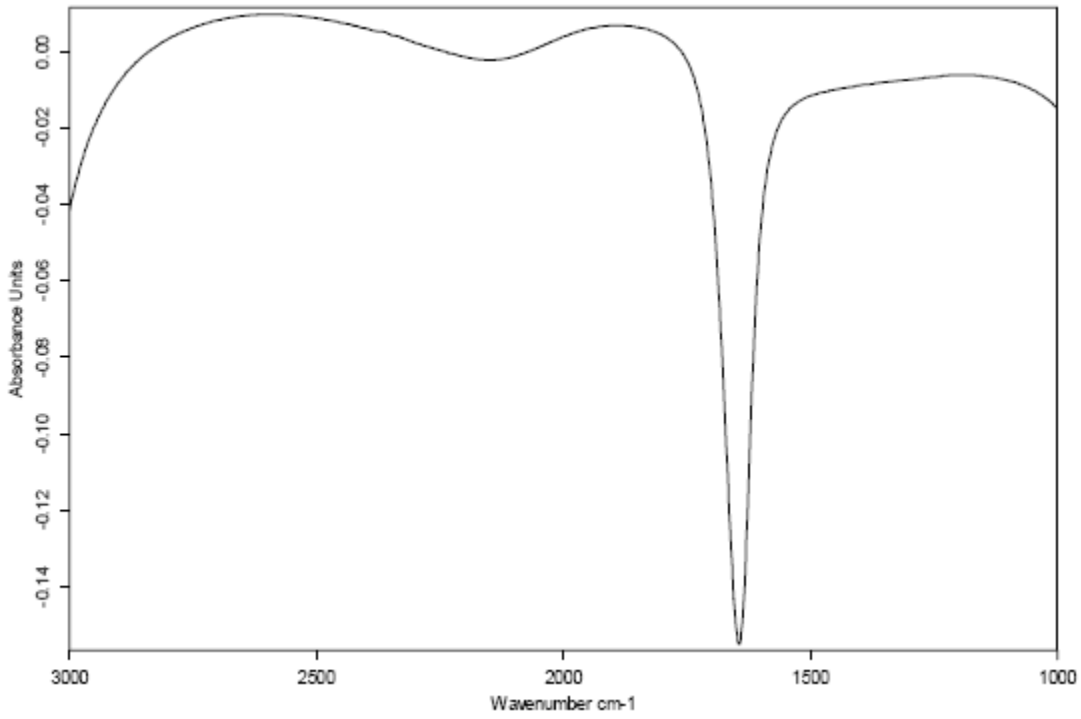

Figure 8: Intensive IR absorption of water.

1.4 My Thesis Project

Recently, Attenuated Total Reflection (ATR) technique has been applied to the IR spectroscopic of proteins/peptides in H_2O solution.[38, 39, 63-68] Unlike the traditional liquid IR cells with path length in millimeter level, the path-length of IR in the sample solution of ATR is only several micrometers, since the incident IR beam is totally reflected within the ATR crystal and penetrates the interface containing the sample by several micrometers via evanescent wave (Figure 9). Therefore, the proof-of-principle experiment to validate the application of ^{13}C isotope-edited FTIR spectroscopy in H_2O by ATR was performed in this thesis.

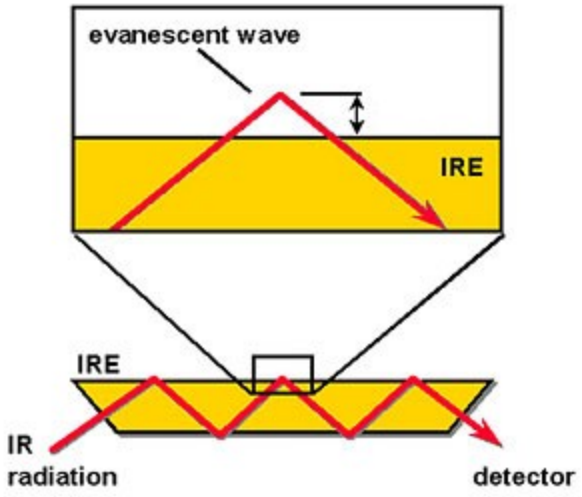

Figure 9: Illustration of the ATR technique.

CHAPTER II

MATERIALS AND METHODS

2.1 Peptide Synthesis

All the peptides in this thesis were synthesized via Solid-Phase Peptide Synthesis (Fmoc) chemistry.[69-71] Unlike ribosomal synthesis, peptides are synthesized artificially from C-terminus to N-terminus. In solid-phase synthesis, peptides are grown on an insoluble polymer (solid support) and the important step in the solid-phase synthesis is the selection of solid support. The solid support used in this research work was Wang resin (made up of polystyrene beads onto which the acid-labile p-hydroxybenzyl alcohol linker is attached) because it has excellent swelling properties, mechanical strength and also feasible cleavage of peptides from it in mild acidic conditions is possible. [70] The peptide synthesis comprises repeated cycles of coupling-washing-deprotection-washing (Figure 10). During the coupling step, the amine group of the free amino acid in N,N-dimethylformide (DMF) solution is protected by fluorenylmethyloxycarbonylchloride (Fmoc) group and the carboxylic group is activated by diisopropylcarbodiimide (DIC). The activated carboxylic group will react with the amine group on the surface of the solid phase to form an amide bond. After the coupling, the remaining free Fmoc-protected amino acid in the DMF solution will be vented. The resin will be washed by fresh DMF to clean up the surface of solid phase. Then, piperidine/DMF mixture solution (1:4 (v/v)) will be added to the reaction vessel to initiate the deprotection. During the deprotection step, Fmoc group which protects the amine group will react and link with piperidine. As a

result, the amine group will be deprotected and ready to couple with the next amino acid. Thus, amino acids will be coupled onto the surface of the resin one by one to form a peptide, which will remain covalently attached to the surface of the resin until cleaved from it by trifluoroacetic acid (TFA).

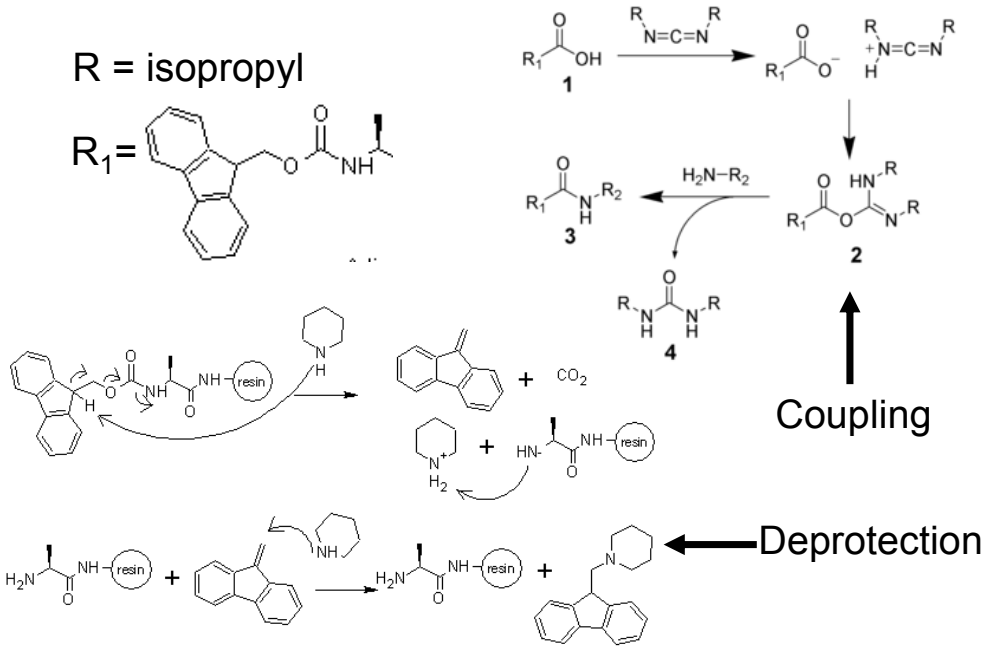

Figure 10: Organic mechanisms of coupling and deprotection in peptide synthesis

2.2 High Performance Liquid Chromatography (HPLC)

HPLC was performed using a solid support stationary phase (also called a "column") containing unmodified silica resins. This technique is now called "normal phase chromatography". In normal phase chromatography, the stationary phase is hydrophilic and therefore has a strong affinity for hydrophilic molecules dissolved in the mobile phase. As a consequence, the hydrophilic molecules in the mobile phase tend to bind (or "adsorb") to the column, while the hydrophobic molecules pass through the

column and are eluted first. For the purification of peptides, the reversed phase HPLC was utilized. The stationary phase of reversed phase HPLC is usually alkyl chain derivatives such as the octadecyl group that is coupled onto the silica resins. Different from the normal phase HPLC, hydrophilic molecules pass through the columns more quickly and are eluted earlier than hydrophobic molecules in RP-HPLC.

The crude peptides (both unlabeled and ^{13}C labeled) were purified by Waters Model 1525 HPLC (Milford, MA) equipped with Model 2489 UV-Vis detector (Figure 11) through a semi-preparative reversed-phase (RP) column (Model Jupiter-00G-4055-P0 of 21.5 mm internal diameter and 250 mm length) from Phenomenex Inc. (Torrance, CA). The eluents were 0.1% trifluoroacetic acid in water (V/V, mobile phase A) and 0.1% trifluoroacetic acid in acetonitrile (V/V, mobile phase B). At a flow rate of 21.5 mL/min, purification of the peptides was accomplished with an elution gradient of 8–16% phase B for 35 minutes at 275 nm wavelength.

Figure 11: Waters Model 1525 HPLC system.

2.3 Mass Spectroscopy

Mass spectrometry works by ionizing chemical compounds to generate molecular ions or molecular fragment ions for measurement according to their mass-to-charge ratios. A mass spectrometer usually consists of three major components: ion source, mass analyzer, and detector. The ion source converts the sample into ions. An extraction system transfers the ions from the sample into the mass analyzer and to the detector. The mass analyzer will separate the ions of various molecules by mass-to-charge ratio. The detector will provide signal intensities for calculating the abundances of each ion present.

All of the mass spectrometric measurements in this thesis were conducted on an Electrospray (ES) −Time of flight (TOF) (Waters Synapt G2 model shown in Figure 12) mass spectrometer (Milford, MA). Both labeled and unlabeled peptides were dissolved in water with 0.5 % trifluoroaceitic acid (TFA). Positive ion mode was used and the capillary voltage is 3 kV. Ion source temperature is 100 °C and N_2 gas used for desolvation was kept at a flow rate of 500 L/hour.

Figure 12: Waters Synapt tandem mass spectrometer with time-of-flight configuration.

2.4 Circular Dichroism (CD) Spectroscopy

The circular dichroism (CD) spectra in this thesis were measured by a JASCO J-810 spectropolarimeter fitted with a 150-W xenon lamp (Figure 13). Quartz cells of 1 mm path length were used for all CD measurements and the spectra were recorded with a response time of 4 s and scan speed of 20 $nm \cdot min^{-1}$ of 2 complete scans.

Figure 13: JASCO J-810 CD spectrometer.

2.5 ATR-FTIR Spectroscopy

The FTIR spectra of labeled and unlabeled peptides aqueous solutions with concentration from 5 to 12 $mg \cdot ml^{-1}$ were measured by the Bruker EQUINOX 55 spectrometer with BioATR-cell II accessory (ZnSe crystal) (Figure 14) on the baseplate A729/q with a resolution of 2 cm^{-1} and co addition of 128 scans. Pure water solution was used as the background for FTIR measurement.

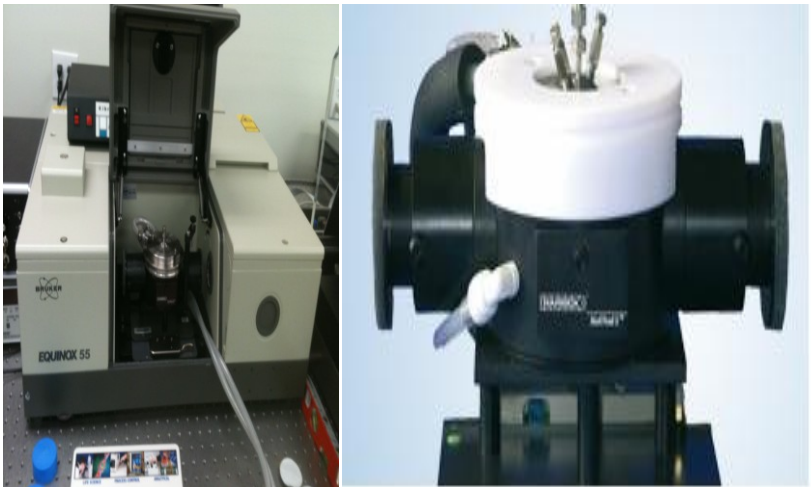

Figure 14: Bruker Equinox 55 spectrometer and Bio-ATR cell II unit.

CHAPTER III

RESULTS

3.1 HPLC Chromatogram of Ac-YAAKAAAAKAAAAKAAH-NH_2 (pep17)

The HPLC chromatogram of unlabeled pep17 is shown in Figure 15. There are four major peaks in the HPLC pattern and only one of the peaks is pep17. All the other peaks may be the unfinished peptide segments. The peak with a retention time of 24.5 minutes is pep17, which was confirmed by the mass spectroscopy (Figure 17). The HPLC chromatogram of the ^{13}C labeled pep17 is almost identical to that of unlabeled pep17 and the result of ^{13}C labeled pep17 at 2&3 residues (L1 in Scheme 1) is shown in Figure 16. The retention time of L1 is also 24.5 minutes and the relative peak intensity of other peaks is higher than those of unlabeled pep17 (Figure 15). This indicates the increasing impurities, which may be because ^{13}C isotopic effect slows down the reaction rate of peptide synthesis and decrease the yield. HPLC pattern of other ^{13}C double labeled pep17 (i.e., L2, L3, and L4) is identical to Figure 16.

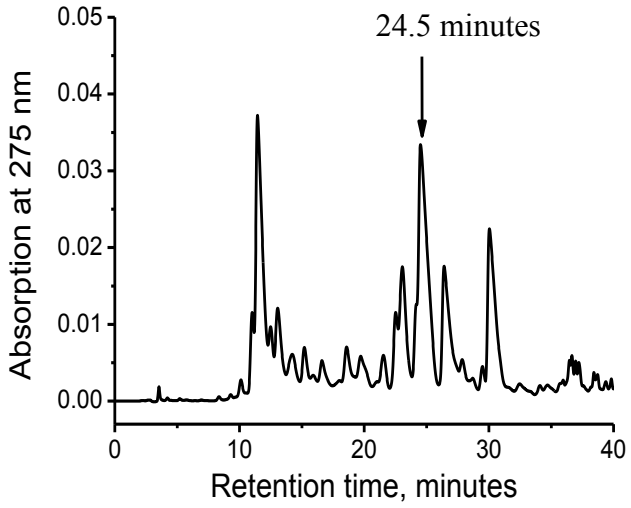

Figure 15: HPLC chromatogram of unlabeled pep17.

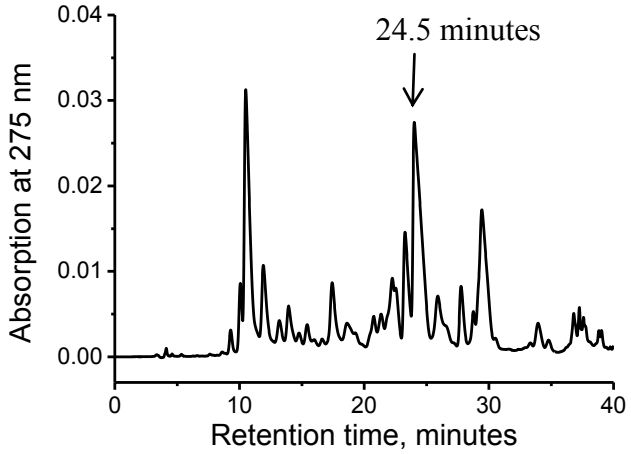

Figure 16: HPLC chromatogram of L1 labeled pep17.

3.2 Mass Spectra of Unlabeled and Labeled Peptides

The purified pep17 by HPLC was analyzed by Mass spectroscopy and the results are shown in Figure 17. The peak appearing at 1556.9 is assigned to the single protonated pep17, whose theoretical molecular weight is 1555.8. The double and triple protonated pep17 show the peaks at 778.9 and 519.6, respectively. As for double ^{13}C labeled pep17 at 2 and 3 residues (e.g., L1 in Scheme 1), the single, double, and triple protonated peaks are at 1558.7, 779.8, and 520.2, respectively, (Figure 18) all of which correlate well to the theoretical value of the peptide molecular mass (i.e., 1557.8). The mass spectra of L2, L3, and L4 are identical to that of L1 as shown in Figure 18. No obvious impurity peak was detected in either Figure 17 or Figure 18. This indicates the purity of both labeled and unlabeled peptides is good.

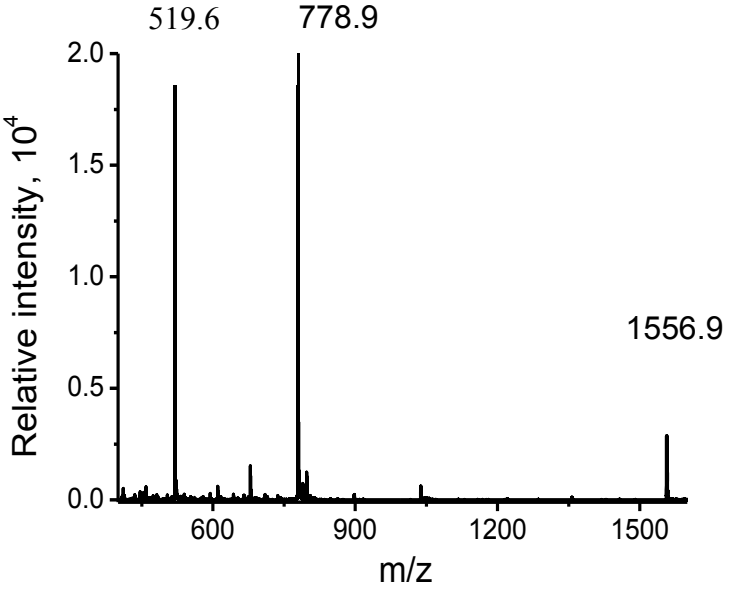

Figure 17: Mass spectra of unlabeled pep17

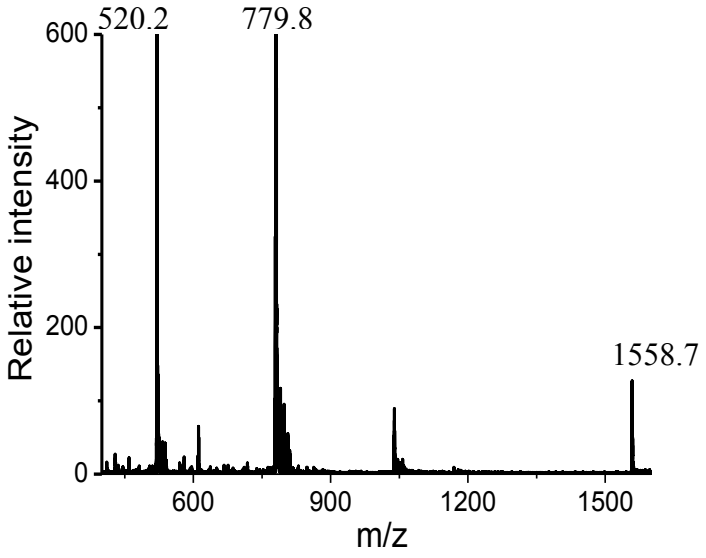

Figure 18: Mass spectra of L1 labeled pep17.

3.3 CD Spectra of Both Unlabeled and Labeled pep17

In order to detect the transformation of pep17, CD spectra of pep17 at various pH values under 5 °C were measured and the results are shown in Figure 19. At pH 13.0, the CD spectrum of unlabeled pep17 showed characteristic peaks (double negative peaks at 208 nm and 222 nm) of α-helix (Figure 19). When pH was decreased to 5.0, the conformation of pep17 was changed to unstructured as indicated by the presence of the negative peak at 199 nm (red curve in Figure 19). In addition, transformation of pep17 was also detected at pH 13.0 under various temperatures. When the temperature was increased, the absolute value of the negative peak intensity at 222 nm (the characteristic peak of α-helix) decreases as shown in Figure 20. This indicates that percentage of α-helix in pep17 decreases with the increase of temperature. The CD spectra of labeled pep17 are identical to those of unlabeled pep17 as shown in Figure 19.

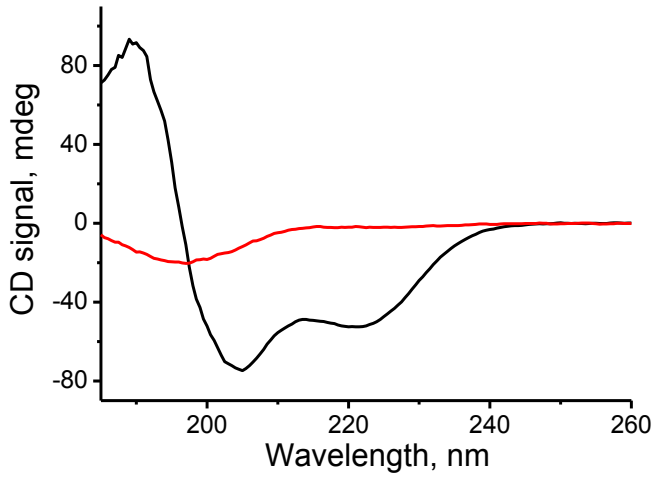

Figure 19: CD spectrum of unlabeled pep17 at pH 5.0 (red curve) and 13.0 (black curve)

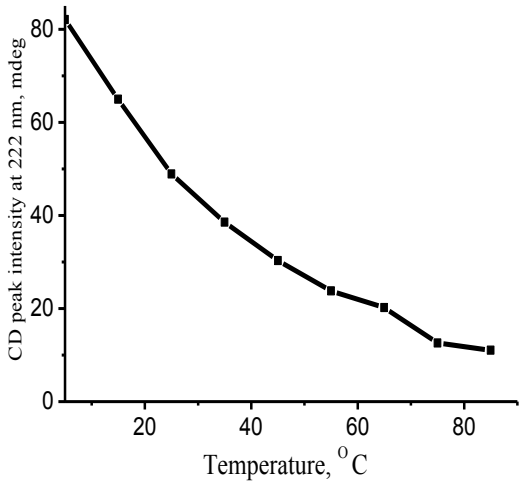

Figure 20: Plot of CD peak intensity as a function of temperature

3.4 ^{13}C Edited ATR-FTIR Spectroscopy of Unlabeled and Labeled pep17

The ATR-FTIR spectra of unlabeled pep17 as well as L2 (^{13}C labeled at 6 and 7 residues) and L3 (^{13}C labeled at 11 and 12 residues) at various temperatures are shown in Figures 21-24. Amide II band was detected around 1540 cm^{-1}, which is normal in H_2O. A broad peak around 1640 cm^{-1} was detected for unlabeled pep17 (Figure 21) together with a shoulder peak at 1675 cm^{-1} at 15 °C. The peak at 1640 cm^{-1} is assigned to unstructured conformation (Table 3). It has been reported that the peak of α-helix depends on the length of helix. For long helix with more than 20 residues, the peak in Amide I band will be around 1647 cm^{-1} and shorter helix will show a peak with higher frequency such as 1665 cm^{-1} (Table 3).[46] Therefore, the peak at 1675 cm^{-1} may be assigned to α-helix because there are only 17 residues in pep17 and the length of helix should be very short. To further confirm this, two experiments were performed.

First, temperature was increased to 25 °C and 45 °C, because the percentage of α-helix decreases as shown by the CD results (Figure 20). The peak intensity decreases as temperature was increased (Figure 22) and consequently, the 1675 cm^{-1} is the peak of α-helix. Second, ATR-FTIR spectrum of unlabeled pep17 was performed in pH 5.0, in which pep17 was unstructured as shown by the CD results above (Figure 19). Only one peak at 1641 cm^{-1} (peak position of unstructured conformation) was detected in Amide I band of unlabeled pep17 (Figure 21). Therefore, the peak at 1675 cm^{-1} can be assigned to α-helix. In addition, L2 (^{13}C labeled pep17 at residues 6 and 7) was also dissolved in aqueous solution at pH 5.0 and the spectrum of L2 is identical to that of unstructured

pep17 (red curve in Figure 22). This indicates that the peak of the ^{13}C labeled residues in unstructured conformation is the same as that of regular unlabeled residues.

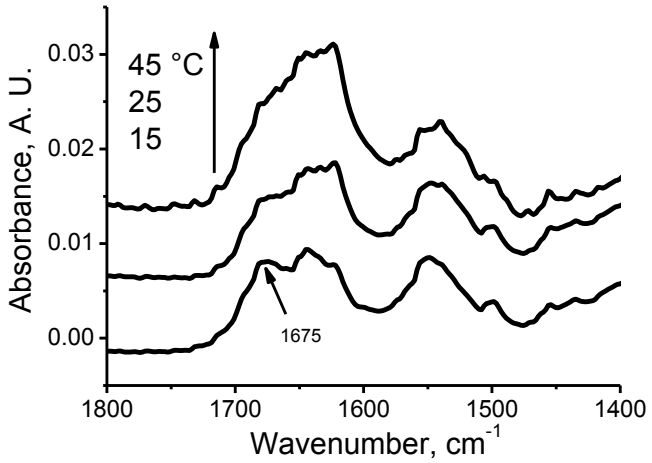

Figure 21: ATR-FTIR spectra of unlabeled peptide at various temperatures

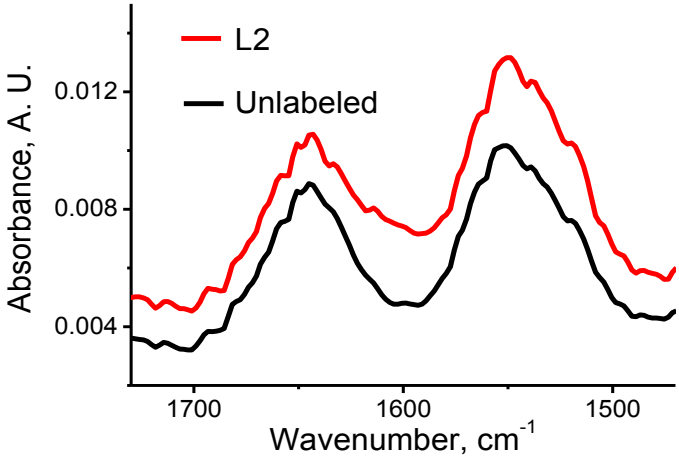

Figure 22: ATR-FTIR spectra of unlabeled and L2 labeled pep17 at pH 5.0

As for the ATR-FTIR spectrum of L2 (Figure 23), the peaks at 1640, 1675, and 1545 cm^{-1} were detected. Another peak at 1602 cm^{-1}, which is not the peak of ^{13}C labeled residues in unstructured conformation as shown in Figure 21, was also detected. Thus, the only possibility is that 1602 cm^{-1} (referred as Amide I' band hereafter) is the fingerprint peak of the ^{13}C labeled residues in α-helix. When the temperature was increased, the peak at 1675 cm^{-1} (the overall peak of α-helix) decreased. However, there was no change in the peak intensity at 1602 cm^{-1}, indicating residues 6 and 7 are still in α-helix even at high temperature (i.e., 45 °C). Similar results were detected for L3 (Figure 24), the peak at 1602 cm^{-1} was detected at 15 °C and did not disappear at 45 °C. Therefore, residues 11 and 12 are also in α-helix at 45 °C**.**

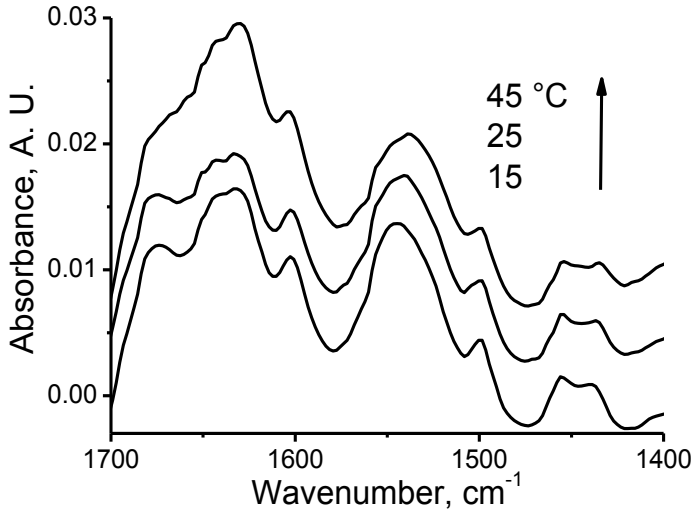

Figure 23: ATR-FTIR spectra of L2 labeled pep17 at various temperatures

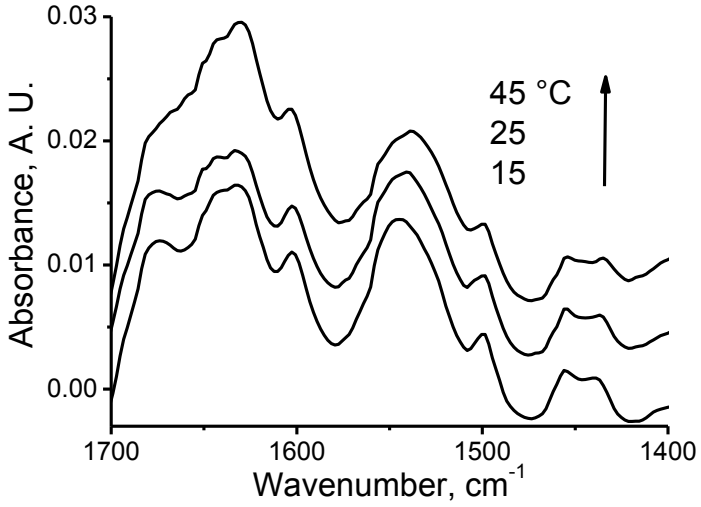

Figure 24: ATR-FTIR spectra of L3 labeled pep17 at various temperatures

3.5. ^{13}C Edited ATR-FTIR Spectra of L1 and L4

The ATR-FTIR spectra of L1 (^{13}C labeled at 2 and 3 residues close to the C-terminus of pep17) and L4 (^{13}C labeled at 15 and 16 residues close to the N-terminus of pep17) are shown in Figure 25 and Figure 26. As for L1, the peak at 1602 cm^{-1} was very weak even at 15 °C (Figure 25). When temperature was increased, the peak completely disappeared. This indicates that residues 2 and 3 are almost unstructured even at 15 °C and this unstructured conformation was maintained when temperature was increased. As for L4, the peak at 1602 cm^{-1} was clearly detected at 15 °C (Figure 26). However, the peak intensity decreased substantially when temperature was increased to 45 °C. Therefore, residues 15 and 16 are in α-helix at 15 °C and were changed to unstructured conformation when the temperature was increased.

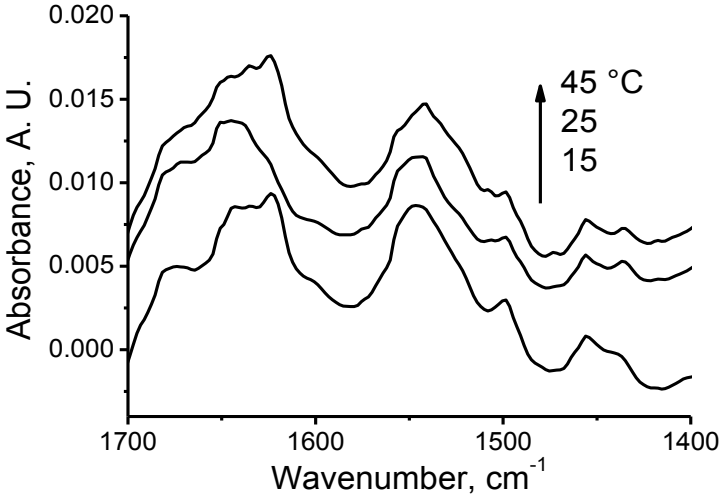

Figure 25: ATR-FTIR spectra of L1 labeled pep17 at various temperatures

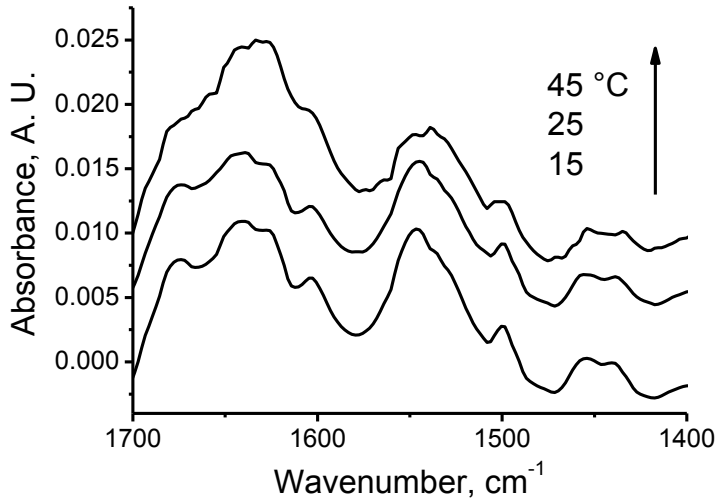

Figure 26: ATR-FTIR spectra of L4 labeled pep17 at various temperatures.

CHAPTER IV

DISCUSSION AND CONCLUSION

4.1 Presence of Amide II Band

As mentioned in Chapter 1, the Amide II band which is related to the bending mode vibration of N-H. In D_2O, Amide II band is shifted to ~1400 cm^{-1} because of the higher atomic weight of deuterium atom. As shown in Figures 21-24, the Amide II band appears at around 1545 cm^{-1}, which is the normal position in H_2O. This is a clear evidence of the success of the measurement of FTIR spectra of pep17 in H_2O by ATR. However, the gap between the Amide I band and the Amide II band is smaller in H_2O than that in D_2O. If the Amide II band overlaps with the Amide I' band from ^{13}C labels, the spectral interpretation will be difficult and it is impossible to apply ^{13}C isotope-edited FTIR in H_2O.

4.2 Amide I' Band of ^{13}C Labeled Residues in Unstructured Conformation

Theoretically, ^{13}C labeled residues will down shift the peak position even for a residue in unstructured conformation. However, in Figure 22, there is no difference in the spectra of unlabeled pep17 and L2 at pH 5.0, a condition in which both of the peptides are in unstructured conformation. This may be due to the fact that solvent (i.e., H_2O) molecules play an important role in unstructured conformation and that the carbonyls in unstructured conformation are surrounded by H_2O molecules. This will decrease the downshifting effect of ^{13}C labels. Therefore, the difference between regular residues and ^{13}C labeled residues in unstructured conformation may be too small to be detected.

4.3 Amide I' Band of ^{13}C Labeled Residues in α-helix

Unlike the residues in the unstructured conformation, carbonyls in α-helix can form strong intra-molecular H-bond. Thus, solvent H_2O molecules do not interact with the carbonyls in α-helix as much and the ^{13}C labels will downshift the Amide I' band substantially. However, if the Amide I' band was downshifted too much and covered by the Amide II band, the detection of Amide I' band would be difficult and the application of ^{13}C isotope-edited FTIR technique in H_2O would be challenging. Fortunately, the Amide I' band of α-helix appears at 1602 cm^{-1}, which is just in the middle of Amide I and Amide II band. Since the background absorbance from unlabeled pep17 is weak at 1602 cm^{-1} (Figure 23), the peak at 1602 cm^{-1} will be easy to detect. The position of the Amide I' band of α-helix at 1602 cm^{-1} without spectral overlap makes it possible for the future application of ^{13}C isotope-edited FTIR technique in analyzing the structure of peptides in H_2O.

4.4 D_2O Effect on the Structure and Biophysical Properties of Proteins

Since D_2O is often used as solvent in the study (such as NMR) of proteins, there has been a longstanding debate on the effect of D_2O on the structure of proteins. Fisher *et al*. have reported that replacement of hydrogen by deuterium (i.e., H/D exchange) can only cause subtle change in the structure of proteins.[59] On the other hand, Sanchez-Gonzalez and co-authors have shown that H/D exchange causes changes in the protein structure of fish surimi.[72] In addition, it has been reported that H/D exchange can cause changes in the stability of some globular proteins.[61]

In this work, C-terminus residues (e.g., residues 2 and 3) are in unstructured conformation and other residues (such as residues 6, 7, 11, 12, 15, and 16) are in α-helix

in H_2O. Our results are exactly the same as previously reported about pep17 in D_2O. However, pep17 is unstructured at pH 5.0 and transforms to α-helix at pH 13.0 in H_2O. This is different from the behavior of pep17 in D_2O, in which pep17 keeps the α-helical conformation from pH 1.0 to 13.0. In general, we can conclude that D_2O changes the structure of pep17 at pH 5.0 significantly and also affects the biophysical properties substantially.

4.5 Conclusion

Unlabeled and ^{13}C labeled pep17 were synthesized. The pep17 samples were confirmed by mass spectroscopy and purified by reversed phase HPLC. Pep17 is in unstructured conformation at pH 5.0 but is transformed to α-helix at pH 13.0. No difference was detected between regular and ^{13}C labeled residues in unstructured conformation. However, the peak of ^{13}C labeled residues in α-helix appears at 1602 cm^{-1}, which can be used as a fingerprint peak of α-helix for specifically ^{13}C labeled residue. For example, no peak at 1602 cm^{-1} was detected although residues 2 and 3 at C-terminus were ^{13}C labeled at pH 13.0. Therefore, residues 2 and 3 are in unstructured conformation even at pH 13.0. On the contrary, other residues are in α-helix at pH 13.0 as revealed by the presence of the peak at 1602 cm^{-1} in the ATR-FTIR spectra. Theoretically, the conformation of all the residues in a peptide can be screened by this method. For the first time, the elucidation of the secondary structure of the pep17 has been demonstrated using the ^{13}C isotope-edited by ATR FTIR in H_2O.

CHAPTER V

FUTURE WORK

5.1 Other Applications of ^{13}C isotope-edited FTIR to Obtain More Detailed Information about the Structure of α-helix

If there are two ^{13}C labeled residues in α-helix, there could be two possible arrangements of the structure. As mentioned above, the regular Amide I band of α-helix (as shown in Scheme 2-A) appears at 1630 cm^{-1} in D_2O, whereas the ^{13}C labeled residue has been reported to shift the Amide I band to 1600 cm^{-1} when forming H-bond with regular residues (Scheme 2-B). The peak at 1600 cm^{-1} was referred as ^{13}C-^{12}C coupling peak. If both neighboring residues contain ^{13}C labeled residues (Scheme 2-C), a strong coupling between ^{13}C=O occurs (referred as ^{13}C-^{13}C coupling) and the wavenumber of Amide I band will be further decreased to 1595 cm^{-1}. This can be used as a fingerprint peak to determine the neighboring residues in helices (i.e., the ^{13}C-^{13}C coupling).[55] If all the neighboring residues have been determined, the structure of α-helix is clarified at residue level as a consequence.

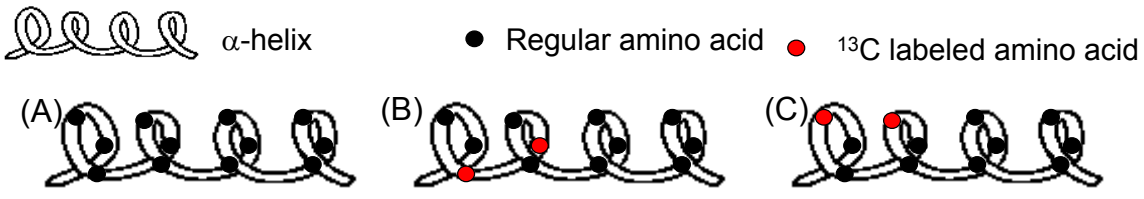

Scheme 2: Hydrogen bond formation between the amide groups in α-helix. The atoms in red are ^{13}C labeled residues.

Decatur *et al.* has used D_2O as a solvent for the ^{13}C isotope-edited FTIR to determine the neighboring residues in α-helix.[55] Our future work is to use the ^{13}C isotope-edited FTIR technique to determine the neighboring residues in α-helix in H_2O. As mentioned in Chapter 3, the α-helix in pep17 is too short and may not be a good model for regular α-helix. Thus, peptide with 25 residues (i.e., $(AAAAK)_4AAAAY$) has been also used as a model peptide of α-helix for a long time and the structure of this peptide has not been clarified in H_2O.[54] Consequently, our future work is to label two residues with ^{13}C in $(AAAAK)_4AAAAY$ (referred as pep25 thereafter) as shown in Scheme 3. The number of residues between the two ^{13}C labeled residues increases from L-1 to L-4.

Ac-AAAAKAAAKA<u>AA</u>AKAAAAKAAAAY-NH_2 (L-1)

Ac-AAAAKAAAK<u>A</u>A<u>A</u>AKAAAAKAAAAY-NH_2 (L-2)

Ac-AAAAKAAAK<u>A</u>AA<u>A</u>KAAAAKAAAAY-NH_2 (L-3)

Ac-AAAAKAA<u>A</u>KAA<u>A</u>AKAAAAKAAAAY-NH_2 (L-4)

Scheme 3: Sequence of the ^{13}C double labeled peptides of pep 25. The carbonyls of underlined residues are replaced by ^{13}C labels.

5.2 HPLC Chromatogram of Unlabeled and Double ^{13}C Labeled pep25

The HPLC chromatogram of unlabeled crude pep25 is shown in Figure 27. The peak with a retention time of 20.0 minutes is pep25, which was confirmed by the mass spectroscopy as shown in Figure 29. The HPLC chromatogram of the ^{13}C labeled pep25 is almost identical to that of unlabeled pep25 and the result of ^{13}C labeled pep25 at residues at 12 and 13 (L-1 in Scheme 3) is shown in Figure 28. The retention time of L-1 is also 20.0 minutes and the relative peak intensities of other peaks are higher than those

of unlabeled peptide (Figure 27) This indicates the increasing impurities, which may be due to the ^{13}C isotopic effect which slows down the reaction rate of peptide synthesis and decreases the yield of pep25 synthesis while contributing to the formation of by-products or impurities. The HPLC chromatograms of other ^{13}C double labeled pep25 are identical to Figure 28.

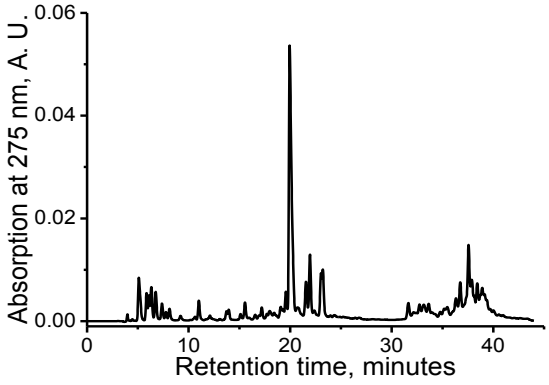

Figure 27: HPLC chromatogram of unlabeled pep25

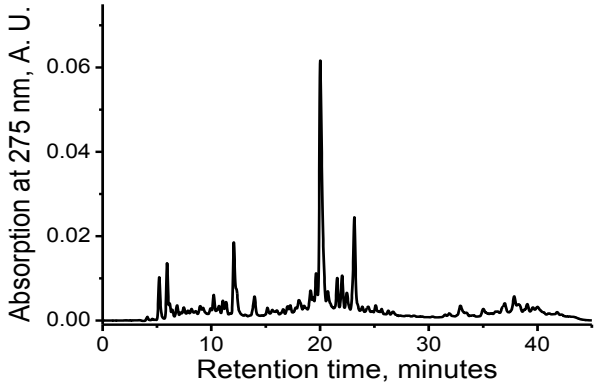

Figure 28: HPLC chromatogram of L-1 labeled pep25

5.3 Mass Spectra of Unlabeled and Labeled pep25

The purified pep25 by HPLC was analyzed by mass spectroscopy and the results are shown in Figure 29. The peak appearing at 1058.4 is assigned to the double protonated pep25, with a theoretical molecular weight of 2115.3. The triple protonated pep25 show the peak at 706.3 and the protonated peak with +4 charge was at 529.7. As for double ^{13}C labeled pep25 at 12 and 13 residues (e.g., L-1 in Scheme 3), the double, triple, and quadruple protonated peaks are at the m/z values of 1059.5, 706.9, and 530.2 respectively, (Figure 30) all of which correlate well to the theoretical value (i.e., 2117.3). The mass spectra of L-2, L-3, and L-4 are identical to that of L-1 as shown in Figure 30.

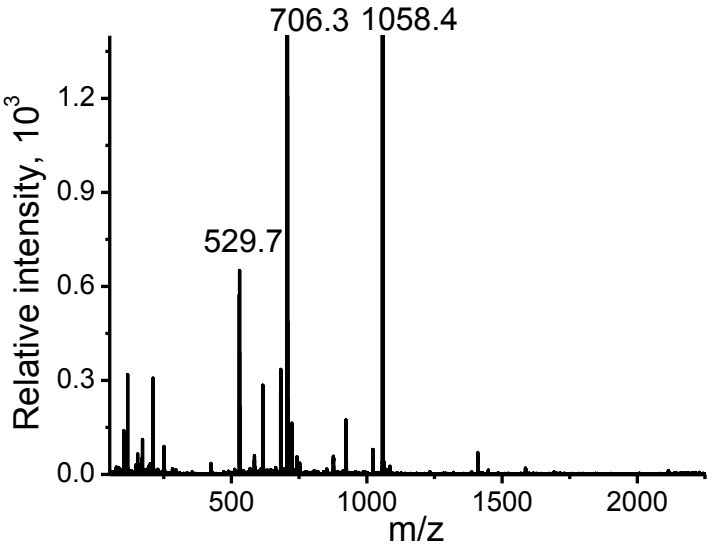

Figure 29: Mass spectra of unlabeled pep25

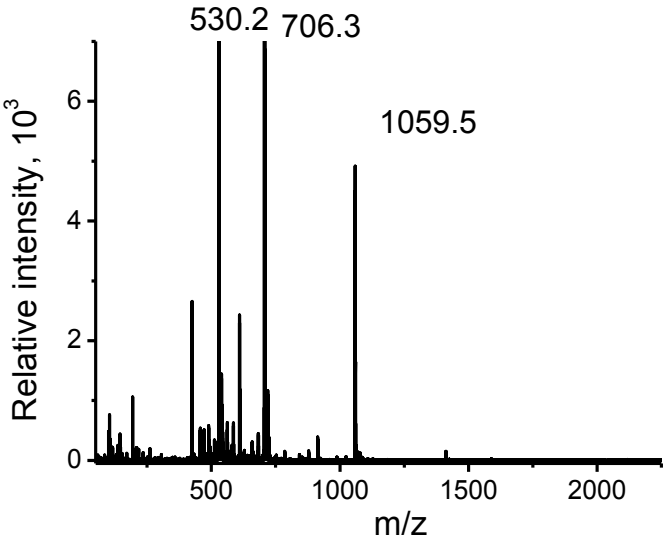

Figure 30: Mass spectra of L-1 labeled pep25

5.4 Future Work Plan on CD and ATR-FTIR Spectroscopic Study of pep25

Although it has been reported that pep25 is in α-helix in acidic and neutral conditions in D_2O, our results in Chapter 3 have shown that D_2O affects the biophysical properties of peptides very much. Therefore, CD spectroscopy of pep25 will be studied under various pH values. The pH value under which pep25 is in α-helix will be chosen for the ATR-FTIR spectroscopic study of unlabeled and ^{13}C labeled pep25. The peak position of both ^{13}C-^{12}C coupling and ^{13}C-^{13}C coupling will be determined. The ^{13}C isotope-edited FTIR will be used to determine the neighboring residues in α-helix in H_2O solution.

REFERENCES

1. Kobko, N.; Paraskevas, L.; del Rio, E.; Dannenberg, J., Cooperativity in amide hydrogen bonding chains: Implications for protein-folding models. *J. Am. Chem. Soc.* **2001,** *123*, 4348-4349.

2. Lam, R. S. H.; Nickerson, M. T., Food proteins: A review on their emulsifying properties using a structure-function approach. *Food Chem.* **2013,** *141* 975-984.

3. Peters, D.; Peters, J., Structure and bonding in proteins: Electron organization in amide unit. *J. Mol. Struct.* **1978,** *50*, 133-145.

4. Sachs, J. N.; Engelman, D. M., Introduction to the membrane protein reviews: The interplay of structure, dynamics, and environment in membrane protein function. *Ann. Rev. Biochem.* **2006,** *75*, 707-712.

5. Greenwald, R. A., Superoxide-dismutase and catalase as therapeutic agents for human diseases, a critical review. *Free Radical Biol. Med.* **1990,** *8*, 201-209.

6. Loredo-Trevino, A.; Gutierrez-Sanchez, G.; Rodriguez-Herrera, R.; Aguilar, C. N., Microbial enzymes involved in polyurethane biodegradation: A review. *J. Polymers Envir.* **2012,** *20*, 258-265.

7. Srikanth, K.; Pereira, E.; Duarte, A. C.; Ahmad, I., Glutathione and its dependent enzymes' modulatory responses to toxic metals and metalloids in fish-a review. *Environ. Sci. Pollut. Res.* **2013,** *20*, 2133-2149

8. Testa, B.; Pedretti, A.; Vistoli, G., Foundation review: Reactions and enzymes in the Metabolism of drugs and other Xenobiotics. *Drug Disc. Today.* **2012,** *17*, 549-560.

9. Wevers, R. A.; de Rijk-van Andel, J. F.; Brautigam, C.; Geurtz, B.; van den Heuvel, L.; Steenbergen-Spanjers, G. C. H.; Smeitink, J. A. M.; Hoffmann, G. F.; Gabreels, F. J. M., A review of biochemical and molecular genetic aspects of tyrosine hydroxylase deficiency including a novel mutation (291delC). *J. Inherited Metabolic Dis.* **1999**, *21*, 364-373.

10. McCauley, M. J.; Williams, M. C., Review: Optical tweezers experiments resolve distinct modes of DNA-protein binding. *Biopolymers.* **2009,** *91*, 265-282

11. Dubnau, D., Binding and transport of transforming DNA by Bacillus subtilis: The role of type-IV pilin-like proteins - A review. *Gene.* **1997,** *192*, 191-198.

12. Appert-Collin, A.; Baisamy, L.; Diviani, D., Review - Regulation of G protein-coupled receptor signaling by A-kinase anchoring proteins. *J. Receptors Sign. Trans.* **2006,** *26*, 631-646.

13. Mizejewski, G. J., Review of the putative cell-surface receptors for alpha-fetoprotein: identification of a candidate receptor protein family. *Tumor Biol.* **2011,** *32*, 241-258.

14. Chautard, E.; Thierry-Mieg, N.; Ricard-Blum, S., Interaction networks: From protein functions to drug discovery. A review. *Path. Biol.* **2009,** *57*, 324-333.

15. Smythies, J.; Galzigna, L., The oxidative metabolism of catecholamines in the brain: a review. *Biochim. Biophys. Acta.* **1998,** *1380*, 159-162.

16. Varadarajan, S.; Yatin, S.; Aksenova, M.; Butterfield, D. A., Review: Alzheimer's amyloid b-peptide-associated free radical oxidative stress and neurotoxicity. *J. Struct. Biol.* **2000,** *130*, 184-208.

17. Wright, J. A.; Brown, D. R., Alpha-synuclein and its role in metal binding: Relevance to Parkinson's disease. *J. Neurosci. Res.* **2008,** *86*, 496-503.

18. Deisenhofer, J.; Epp, O.; Miki, K.; Huber, R.; Michel, H., Structure of the protein subunits in the photosynthetic reaction centre of Rhodopseudomonas viridis at 3Å resolution. *Nature.* **1985,** *318*, 918-924.

19. Petry, S.; Brodersen, D. E.; Murphy, F. V.; Dunham, C. M.; Selmer, M.; Tarry, M. J.; Kelley, A. C.; Ramakrishnan, V., Crystal structures of the ribosome in complex with release factors RF1 and RF2 bound to a cognate stop codon *Cell.* **2005,** *123*, 1255-1266.

20. Pfister, P.; Corti, N.; Hobbie, S.; Bruell, C.; Zarivach, R.; Yonath, A.; Bottger, E. C., 23S rRNA base pair 2057-2611 determines ketolide susceptibility and fitness cost of the macrolide resistance mutation 2058A -> G. *Proc. Natl. Acad. Sci. U. S. A.* **2005,** *102*, 5180-5185.

21. Steitz, T. A., A structural understanding of the dynamic ribosome machine. *Nat. Rev. Mol. Cell Biol.* **2008,** *9*, 242-253.

22. Adessi, C.; Soto, C., Beta-sheet breaker strategy for the treatment of Alzheimer's disease. *Drug Development Res.* **2002,** *56*, 184-193.

23. Pauling, L.; Corey, R. B., Configurations of polypeptide chains with favored orientations around single bonds. *Proc. Nat. Acad. Sci. U.S.A.* **1951,** *37*, 729-740.

24. Wang, C.; Shah, N.; Thakur, G.; Zhou, F.; Leblanc, R. M., a-Synuclein in a-helical conformation at the air-water interface: Implication of conformation and orientation changes during its accumulation/aggregation. *Chem. Commun.* **2010,** *46*, 6702-6704.

25. Floudas, C. A.; Fung, H. K.; McAllister, S. R.; Monnigmann, M.; Rajgaria, R., Advances in protein structure prediction and de novo protein design: A review. *Chem. Engin. Sci.* **2006,** *61*, 966-988.

26. Robinson, N. E.; Robinson, A. B., Review article: Use of Merrifield solid phase peptide synthesis in investigations of biological deamidation of peptides and proteins. *Biopolymers.* **2008,** *90*, 297-306.

27. Kahn, R.; Carpentier, P.; Berthet-Colominas, C.; Capitan, M.; Chesne, M. L.; Fanchon, E.; Lequien, S.; Thiaudiere, D.; Vicat, J. Z., P.; Stuhrmann, H., Feasibility and review of anomalous X-ray diffraction at long wavelengths in materials research and protein crystallography. *J. Synchront. Rad.* **2000,** 7, 131-138.

28. Lanyi, J. K., X-ray diffraction of bacteriorhodopsin photocycle intermediates (Review). *Mol. Membrane Biol.* **2004,** *21*, 143-150.

29. Munte, C. E.; Erlach, M. B.; Kremer, W.; Koehler, J.; Kalbitzer, H. R., Distinct conformational states of the Alzheimer -amyloid peptide can be detected by high-pressure NMR spectroscopy. *Angew. Chem.* **2013,** *52*, 8943-8947.

30. Comellas, G.; Rienstra, C. M., Protein structure determination by magic-angle spinning solid-state NMR, and Insights into the formation, structure, and stability of amyloid fibrils. *Ann. Rev. Biophys.* **2013,** *42*, 515-536.

31. Scheidt, H. A.; Morgado, I.; Huster, D., Solid-state NMR reveals a close structural relationship between amyloid-b protofibrils and oligomers. *J. Biol. Chem.* **2012,** *287*, 22822-22826.

32. Scheidt, H. A.; Morgado, I.; Rothemund, S.; Huster, D., Dynamics of amyloid beta fibrils revealed by solid-state NMR. *J. Biol. Chem.* **2012,** *287*, 2017-2021.

33. Fawzi, N. L.; Ying, J. F.; Ghirlando, R.; Torchia, D. A.; Clore, G. M., Atomic-resolution dynamics on the surface of amyloid-beta protofibrils probed by solution NMR. *Nature.* **2011,** *480*, 268-U161

34. Aronoff-Spencer, E.; Burns, C. S.; Avdievich, N. I.; Gerfen, G. J.; Peisach, J.; Antholine, W. E.; Ball, H. L.; Cohen, F. E.; Prusiner, S. B.; Millhauser, G. L., Identification of the Cu^{2+} binding sites in the N-terminal domain of the prion protein by EPR and CD spectroscopy. *Biochemistry.* **2000,** *39*, 13760-13771.

35. Ji, X.; Zheng, J.; Xu, J.; Rastogi, V. K.; Cheng, T.; DeFrank, J. J.; Leblanc, R. M., (CdSe)ZnS quantum dots and organophosphorus hydrolase bioconjugate as biosensors for detection of paraoxon. *J. Phys. Chem. B.* **2005,** *109*, 3793-3799.

36. Constantine, C. A.; Gattas-Asfura, K. M.; Mello, S. V.; Crespo, G.; Rastogi, V.; Cheng, T.; De Frank, J. J.; Leblanc, R. M., Layer-by-layer films of chitosan, organophosphorus hydrolase and thioglycolic acid-capped CdSe quantum dots for the detection of paraoxon. *J. Phys. Chem. B.* **2003,** *107*, 13762-13764.

37. Sreerama, N.; Woody, R. W., Estimation of protein secondary structure from CD spectra: Comparison of CONTIN, SELCON and CDSSTR methods with an expanded reference set. *Anal. Biochem.* **2000,** *282*, 252-260.

38. Wang, C.; Micic, M.; Ensor, M.; Daunert, S.; Leblanc, R. M., Infrared reflection-absorption spectroscopy and polarization-modulated infrared reflection-absorption spectroscopy studies of the aequorin Langmuir monolayer. *J. Phys. Chem. B.* **2008,** *112*, 4146-4151.

39. Wang, C.; Zheng, J.; Zhao, L.; Rastogi, V. K.; Shah, S. S.; DeFrank, J. J.; Leblanc, R. M., Infrared reflection-absorption spectroscopy and polarization-modulated Infrared Reflection-Absorption Spectroscopy studies of the organophosphorus acid anhydrolase Langmuir monolayer. *J. Phys. Chem. B.* **2008,** *112*, 5250-5256.

40. Hasegawa, T.; Nishijo, J.; Watanabe, M.; Umemura, J.; Ma, Y.; Sui, G.; Huo, Q.; Leblanc, R. M., Characteristics of long-chain fatty acid monolayers studied by infrared external-reflection spectroscopy. *Langmuir.* **2002**, *12*, 4758-4764.

41. Thakur, G.; Leblanc, R. M., Conformation of lysozyme Langmuir monolayer studied by Infrared Reflection Absorption Spectroscopy. *Langmuir.* **2009,** *25*, 2842-2849.

42. Thakur, G.; Micic, M.; Leblanc, R. M., Surface chemistry of Alzheimer's disease: A Langmuir monolayer approach *Colloid. Surf. B.* **2009,** *74*, 436-456.

43. Wang, C.; Zheng, J.; Oliveira, O. N.; Leblanc, R. M., Nature of the interaction between a peptidolipid Langmuir monolayer and paraoxon in the subphase. *J. Phys. Chem. C.* **2007,** *111*, 7826-7833.

44. Du, X.; Miao, W.; Liang, Y., IRRAS studies on chain orientation in the monolayers of amino acid amphiphiles at the air-water interface depending on metal complex and hydrogen bond formation with the headgroups. *J. Phys. Chem. B.* **2005,** *109*, 7428-7434.

45. Jiang, D.; Dinh, K. L.; Tuthenburg, T. C.; Zhang, Y.; Su, L.; Land, D. P.; Zhou, F., A kinetic model for b-amyloid adsorption at the air/solution interface and its implication to the b-amyloid aggregation process. *J. Phys. Chem. B.* **2009,** *113*, 3160-3168.

46. Dziri, L.; Desbat, B.; Leblanc, R. M., Polarization-modulated FT-IR spectroscopy studies of acetylcholinesterase secondary structure at the air-water interface. *J. Am. Chem. Soc.* **1999,** *121*, 9618-9625.

47. Hasegawa, T.; Moriya, D.; Kakuda, H.; Li, C.; Orbulescu, J.; Leblanc, R. M., Fibril-like aggregate formation of peptide carboxylate Langmuir films analyzed by surface pressure, surface dipole moment, and infrared spectroscopy. *J. Phys. Chem. B.* **2005,** *109*, 12856-12860.

48. Zheng, J. Y.; Constantine, C. A.; Zhao, L.; Rastogi, V. K.; Cheng, T. C.; DeFrank, J. J.; Leblanc, R. M., Molecular interaction between organophosphorus acid anhydrolase and diisopropylfluorophosphate. *Biomacromolecule.* **2005,** *6*, 1555-1560.

49. Dong, A.; Huang, P.; Caughey, W., Redox-dependent changes in β-extended chain and turn structures of cytochrome c in water solution determined by second derivative Amide I infrared spectra. *Biochemistry.* **1992,** *31*, 182-189.

50. Halverson, K. J.; Sucholeiki, I.; Ashburn, T. T.; Lansbury, P. T., Location of b-sheet-forming sequences in amyloid proteins by FTIR. *J. Am. Chem. Soc.* **1991,** *113*, 6701-6703.

51. Haris, P. I.; Robillard, G. T.; van Dijk, A. A.; Chapman, D., Potential of carbon-13 and nitrogen-15 labeling for studying protein-protein interactions using Fourier-transform infrared spectroscopy. *Biochemistry.* **1992,** *31*, 6279-6284.

52. Tadesse, L.; Nazarbaghi, R.; Walters, L., Isotopically enhanced infrared spectroscopy: a novel method for examining secondary structure at specific sites in conformationally heterogeneous peptides. *J. Am. Chem. Soc.* **1991,** *113*, 7036-7037.

53. Zhang, M.; Fabian, H.; Mantsch, H. H.; Vogel, H. J., Isotope-edited Fourier transform infrared spectroscopy studies of Calmodulin's interaction with its target peptides. *Biochemisty.* **1994,** *33*, 10883-10888.

54. Barber-Armstrong, W.; Donaldson, T.; Wijesooriya, H.; Gangani, R. A.; Silva, D.; Decatur, S. M., Empirical relationships between isotope-edited IR spectra and helix geometry in model peptides. *J. Am. Chem. Soc.* **2004,** *126*, 2339-2345.

55. Decatur, S. M., Elucidation of residue-level structure and dynamics of polypeptides via isotopp-edited infrared spectroscopy. *Acc. Chem. Res.* **2006,** *39*, 169-175.

56. Decatur, S. M.; Antonic, J., Isotope-edited infrared spectroscopy of helical peptides. *J. Am. Chem. Soc.* **1999,** *121*, 11914-11915.

57. Petty, S. A.; Decatur, S. M., Experimental evidence for the reorganization of b-strands within aggregates of the Ab(16-22) peptide. *J. Am. Chem. Soc.* **2005,** *127*, 13488-13489.

58. http://en.wikipedia.org/wiki/Heavy_water. (Accessed on Sep 20, 2013)

59. Fisher, S. J.; Helliwell, J. R., An investigation into structural changes due to deuteration. *ACTA Crystallogr. A.* **2008,** *64*, 359-367.

60. Kushner, D. J.; Baker, A.; Dunstall, T. G., Pharmacological uses and perspectives of heavy water and deuterated compounds. *Can. J. Physiol. Pharmacol.* **1999,** *77*, 79-88.

61. Efimova, Y. M.; Haemers, S.; Wierczinski, B.; Norde, W.; van Well, A. A., Stability of globular proteins in H_2O and D_2O. *Biopolymers.* **2007,** *85*, 264-273.

62. http://webbook.nist.gov/cgi/cbook.cgi?ID=C7732185&Units=SI&Type=IR-SPEC&Index=1#IR-SPEC. (Accessed on September 20, 2013)

63. Valenti, L. E.; Paci, M. B.; De Pauli, C. P.; Giacomelli, C. E., Infrared study of trifluoroacetic acid unpurified synthetic peptides in aqueous solution: Trifluoroacetic acid removal and band assignment. *Anal. Biochem.* **2009,** *410*, 118-123.

64. Hassler, N.; Baurecht, D.; Reiter, G.; Fringeli, U. P., n Situ FTIR ATR spectroscopic study of the interaction of immobilized human serum albumin with cholate in aqueous environme. *J. Phys. Chem. C.* **2011,** *115*, 1064-1072.

65. Cai, P.; Flach, C. R.; Mendelsohn, R., An infrared reflection-absorption spectroscopy study of the secondary structure in (KL4)(4)K, a therapeutic agent for respiratory distress syndrome, in aqueous monolayers with phospholipids. *Biochemistry.* **2003,** *42*, 9446-9452.

66. Ramajo, A. P.; Petty, S. A.; Starzyk, A.; Decatur, S. M.; Volk, M., The a-helix folds more rapidly at the C-terminus than at the N-terminus. *J. Am. Chem. Soc.* **2005,** *127*, 13784-13785

67. Petty, S. A.; Decatur, S. M., Intersheet rearrangement of polypeptides during nucleation of β-sheet aggregates. *Proc. Nat. Acad. Sci. U.S.A.* **2005,** *102*, 14272-14277

68. Starzyk, A.; Barber-Armstrong, W.; Sridharan, M.; Decatur, S. M., Spectroscopic evidence for backbone desolvation of helical peptides by 2,2,2-trifluoroethanol: An isotope-edited FTIR study. *Biochemistry.* **2005,** *44*, 369-376.

69. Fields, G. B., *Methods in Enzymology*. Academic Press Inc.: New Yorker, 1997.

70. Kates, S. A.; Albericio, F., *Solid-Phase Synthesis, a Practical Guide*. Marcel Dekker, Inc.: New York, 2000.

71. Fields, G. B.; Noble, R. L., Solid-phase peptide synthesis utilizing 9-flourenylmethoxycarbonyl amino acids. *Int. J. Pept. Prot. Res.* **1990,** *35*, 161-214.

72. Sanchez-Gonzalez, I.; Carmona, P.; Moreno, P.; Borderias, J.; Sanchez-Alonso, I.; Rodriguez-Casado, A.; Careche, M., Protein and water structural changes in fish surimi during gelation as revealed by isotopic H/D exchange and Raman spectroscopy. *Food Chem.* **2008,** *106*, 56-64.